Self-trapping of ''necklace-ring'' beams in self-focusing Kerr media

Marin Soljačić[1] and Mordechai Segev[2,3]
[1]*Physics Department, Princeton University, Princeton, New Jersey 08544*
[2]*Physics Department, Technion-Israel Institute of Technology, Haifa 32000, Israel*
[3]*Electrical Engineering Department, Princeton University, Princeton, New Jersey 08544*
(Received 6 October 1999; revised manuscript received 27 March 2000)

Recently, we suggested a type of self-trapped optical beams that can propagate in a stable form in $(2+1)D$ self-focusing Kerr media: Necklace-ring beams [M. Soljačić, S. Sears, and M. Segev, Phys. Rev. Lett. **81**, 4851 (1998)]. These self-trapped necklaces slowly expand their ring diameter as they propagate as a result of a net radial force that adjacent ''pearls'' (azimuthal spots) exert on each other. Here, we revisit the self-trapped necklace beams and investigate their properties analytically and numerically. Specifically, we use two different approaches and find analytic expressions for the propagation dynamics of the necklace beams. We show that the expansion dynamics can be controlled and stopped for more than 40 diffraction lengths, making it possible to start thinking about interaction-collision phenomena between self-trapped necklaces and related soliton effects. Such self-trapped necklace-ring beams should also be observable in all other nonlinear systems described by the cubic $(2+1)D$ nonlinear Shrödinger equation—in almost all nonlinear systems in nature that describe envelope waves.

PACS number(s): 42.65.Tg, 41.20.Jb

I. INTRODUCTION

In recent years, solitons in $(2+1)D$ have drawn significant attention in optics [1], as well as in other fields of physics [2]. Most often, envelope scalar waves in $(2+1)D$, propagating in isotropic media can be described by nonlinear Schrödinger equation (NLSE) [3]. This equation is just the paraxial slowly varying wave equation modified by an additional nonlinear term; thus, its universality particularly for envelope solitons is not surprising. If in addition, the medium is centrosymmetric, and only the lowest-order nonlinearity is important, the system can be modeled by the $(2+1)D$ cubic NLSE. Because of its universality, this equation models very many physical systems. Consequently, it would be desirable to have $(2+1)D$ bright solitons in this equation. Unfortunately, for a long time all known solitons of this equation were thought to be unstable [4]. Nevertheless, recently we were able to construct stable self-trapped bright beams in $(2+1)D$ cubic self-focusing NLSE [5], so-called necklace-ring beams, and their existence as stable entities propagating in Kerr media was shown experimentally [6,7]. Necklace beams are beams shaped like rings, whose intensity is azimuthally periodically modulated as in Fig. 1. In our first paper on this subject [5] we have demonstrated the existence of self-trapped necklaces numerically, and demonstrated their stability to numerical noise. Here we show analytically how to predict and control the radial dynamics of necklace beams, and present analytic solutions for necklace beams in several parameter regimes.

This paper is organized as follows. In Sec. II we provide a brief introduction to necklace beams. In Sec. III we describe a procedure that facilitates control over the instantaneous radial velocity of any necklace. In Sec. IV we present analytical solutions to necklace beams in some specific regimes of parameters as a function of the propagation distance. This enables a direct prediction of the radial acceleration of a necklace when its radial velocity is manipulated. However, this solution works well only in a limited range of necklace parameters. Consequently, in Sec. V we present a different analytical technique that allows one to predict the dynamics of any necklace as a function of its initial parameters. This technique can also predict what happens with the dynamics of the necklace once we manipulate the necklace's instantaneous radial velocity. However, the technique from Sec. V gives us no information whatsoever about the instantaneous necklace shape. In Sec. VI we conclude by summarizing our predictions and propose new experiments.

II. WHAT ARE NECKLACE-RING BEAMS?

In the optics community, it was a commonly held belief that physical systems described by $(2+1)D$ cubic self-focusing NLSE cannot be used for soliton observations since all known self-trapped beams in such systems were thought to be unstable. For example, cylindrically symmetric solutions of all orders of this equation [8] suffer from catastrophic collapse (or diffraction, depending on their power) [4,9]; i.e., any small deviation from the equilibrium shape makes them contract to a point, or diffract to infinity. Since solitons of $(1+1)D$ cubic self-focusing NLSE are known to be stable, one might think that a beam that is self-trapped (a soliton) in one transverse dimension (say, x) and uniform in the other transverse dimension (y), while propagating along z, should be stable. Unfortunately, such a beam is also unstable: it suffers from transverse modulation instability [10]. Small perturbations in the transverse direction [which was initially uniform (y)], grow on top of the pulse as the pulse propagates, and the pulse eventually disintegrates. Similarly, cylindrically symmetrical rings (of radius large compared to their thickness,) suffer from modulation instability in the azimuthal direction, both when they do carry topological charge, and also when they do not [11,12].

Nevertheless, it was shown that beams in planar Kerr-nonlinear waveguides can be accurately described by (1

 ©2000 The American Physical Society

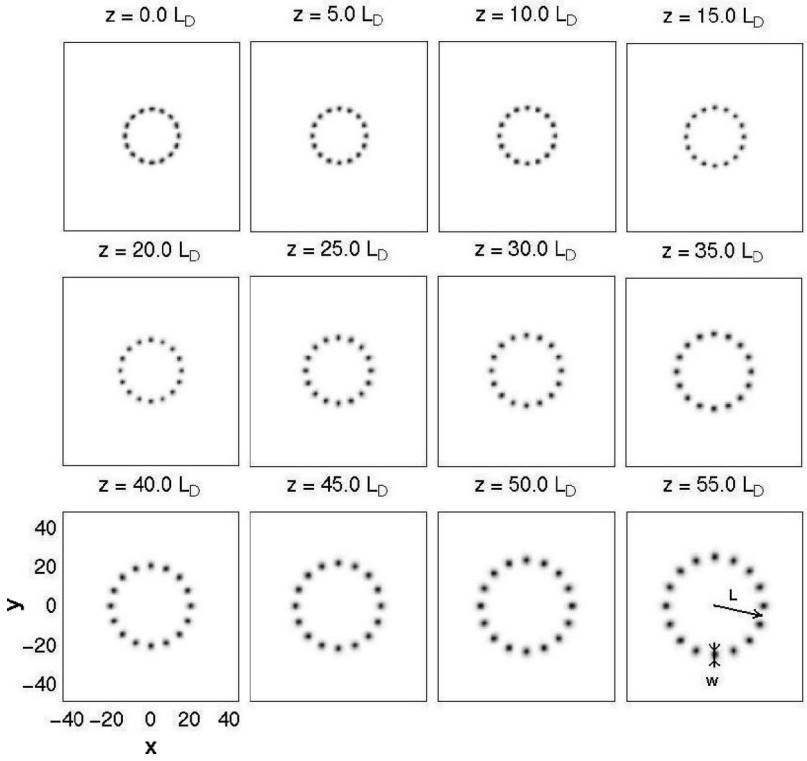

FIG. 1. Example of evolution of a necklace beam with initial shape given by $\psi(r,\theta,z) = \alpha\cos(\Omega\theta)\mathrm{sech}[(r-L)/w]$, where $\alpha=1$, $w=1$, $\Omega=8$, and $L/\Omega=1.707$. The necklace slowly expands as it propagates. The axes are the same for all plots. Dark color indicates high intensity. In all figures in this paper, contrast is enhanced for better clarity.

$+1)D$ cubic self-focusing NLSE as long as the dimension of the beam parallel to the plates (the trapping direction) is much larger than the distance between the plates [13]; thus, solitons of such a configuration are stable. In fact, in 1985, Barthelemy *et al.* have produced the first optical spatial Kerr solitons using an idea that was driven by this understanding [14]. They superimposed two beams that were both narrow in one transverse direction (x), uniform in the other transverse direction, but propagating at a small angle with respect to each other, thus producing an interference pattern in the direction in which each of the beams by itself was uniform (the y direction). The self-focusing Kerr nonlinearity translated the interference grating into a periodic modulation of the index. The spatial wavelength of this modulation was much smaller than the beam's width in x. Therefore, at a proper intensity, the structure self-trapped in x (each beam created a soliton in x), whereas in y the nonlinearity effectively produced a nonlinearly-induced multiple waveguide structure from each of the interference fringes. Because the y width of each induced-waveguide was much narrower than the soliton width (in x), the structure was stable and no transverse instability was observed in y.

Unfortunately, experimentally, neither of the beams could be infinite in the transverse direction. Consequently, the beams eventually walked off from each other and stopped interfering, thereby destroying the configuration. In addition, the described solution is not completely satisfactory since the shapes produced are really only $(1+1)D$ shapes. Clearly, one would like to have higher dimension solitons, which would enable exploring 2D soliton interactions and other interesting features of higher dimensionality.

In Ref. [5] we have built on the idea described in the previous paragraph (and in Ref. [14]) to produce stable self-trapped beams in $(2+1)D$ Kerr media. In our imagination, we took the shapes described in the previous paragraph, and wrapped them around their own tails, thus producing necklace beams [5]. Necklace beams are beams shaped like rings, whose radius is large compared to their radial thickness. In order to avoid modulation instability in the azimuthal direction, the intensity is periodically modulated in the azimuthal direction [like the interference pattern between the $(1+1)D$ solitons of [14]]. An example of a self-trapped necklace beam is shown in Fig. 1. Such a shape can be thought of as a superposition of two equal uniform-intensity rings carrying the same but opposite charges, thus resulting in an interference pattern in the azimuthal direction.

In general, propagation of a necklace beam is not stationary: the beams exhibit slow radial expansion as they propagate. The expansion is a result of a net radial ''force'' that results from the azimuthally alternating phase, and is typically much slower than diffractive expansion. In some cases the nonlinear expansion is even negligible over all propagation distances of experimental interest.

The main feature of necklace beams is that the radial dynamics rate of necklaces is typically many orders of magnitude slower than the rate at which each of the pearls of the necklace would suffer catastrophic collapse if it were standing by itself. In other words, the necklace-ring beam exhibits stationary propagation for a very large distance, during which neither the ring diameter nor the width of each spot (''pearl'') on the ring change significantly. For, example, consider Fig. 1, where after $55L_D$, the radius of the necklace grew by less than a factor of 2. In contrast, each pearl (if standing by itself) undergoes catastrophic collapse (or diffraction) within only a few L_D. (Please see the Appendix.) Therefore, with interactions (collisions) between necklace-ring ''solitons'' in mind, two self-trapped necklaces can mutually interact over a large distance during which they do not change their shapes appreciably. Thereby, one can use necklace-ring self-trapped beams to explore nonlinear inter-

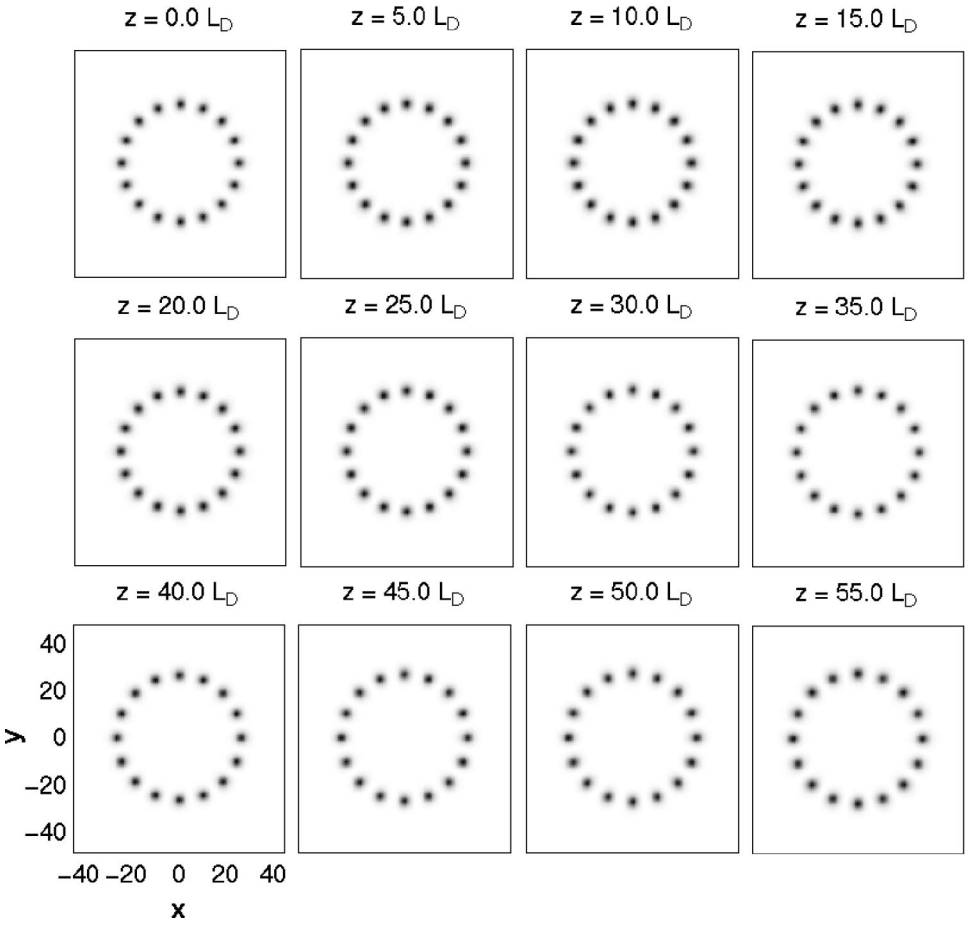

FIG. 2. Stopping the necklace's instantaneous radial velocity. We take the necklace at the output of Fig. 1, and measure its instantaneous radial velocity v_0. Then we multiply the whole shape with $\exp(-iv_0 r)$. The subsequent instantaneous radial velocity drops to 2% of the initial value.

action phenomena and collisions (which are the most fascinating features of all solitons), in $(2+1)D$; this was previously thought to be undoable in $(2+1)D$ self-focusing Kerr media (i.e., in a medium represented by the cubic self-focusing NLSE).

III. CONTROLLING THE EXPANSION RATE OF THE SELF-TRAPPED NECKLACE BEAMS

As shown in [5] necklaces typically grow as they propagate. The intuition behind this growth is that the amplitudes of the neighboring pearls are π out of phase, thereby repelling each other [1,15]; consequently there is a net radial force outwards on each pearl. For numerous reasons, it is important to have a means to control the expansion of the necklace-ring self-trapped beam. For example, it would be nice to be able to stop the expansion, and perhaps even reverse it, at least for some finite propagation distance. In fact, there is a natural way to obtain precisely this goal. Namely, one can take the necklace at any given propagation distance z, and multiply the whole shape with $\exp(-i\Omega r)$, where r is the radial coordinate. Imposing such a radial (transverse) phase influences the radial velocity of each pearl. If the radial velocity of a pearl before applying the radial phase is v, then after the application of the phase, the net radial velocity is roughly v-Ω. Therefore, the instantaneous expansion velocity can be reduced to zero. Furthermore, one can even reverse this velocity so that the necklace immediately after the application of the radial phase initially shrinks. This tool provides control over the instantaneous necklace radius growth. Such a radial phase is trivial to impose experimentally: one just shines a necklace through a ''sharpened pencil'' phase object, made from glass.

The fact that we can produce a shrinking necklace in this manner is not inconsistent with the intuition that the neighboring pearls should repel each other. The procedure we have just suggested to make a shrinking necklace does not in general make the radial acceleration negative, and thus does not turn the repulsion between adjacent ''pearls'' into attraction. To illustrate the idea, consider a necklace with 16 pearls, as we show in Fig. 1, and let it propagate for a while. After $55L_D$, we measure its instantaneous radial velocity v_0, and multiply the whole shape with $\exp(-iv_0 r)$. As one can see in Fig. 2, the instantaneous velocity is significantly reduced. A more careful measurement shows that the reduction in this particular case was from v_0 to approximately -2% of v_0. However, the instantaneous radial acceleration stays positive, so the radial velocity of the necklace keeps increasing even after the application of the radial phase, as shown in Fig. 2. In the subsequent sections we analyze analytically what exactly happens with the radial acceleration as a result of the application of such a radial phase.

IV. APPROXIMATE ANALYTIC SOLUTIONS

In this section we use the action minimization approach in order to obtain an approximate analytical solution to the necklace shape as a function of the propagation distance z. The solution we find works well only in certain regimes of necklace parameters. However, in these regimes it gives an

excellent prediction for the radius of a necklace, the shape of the necklace, and its radial velocity as a function of the propagation distance. It also provides us with a quantitative understanding about what happens with the necklace once we multiply it with a radial phase, as proposed in Sec. III.

We seek an approximate analytic solution in the regime where the radius of the necklace L, is much larger than its thickness w, as defined in the last plot of Fig. 1. In addition, we consider only the cases where the thickness of the necklace w is much larger than the rate of the azimuthal variation $L\pi/(4\Omega)$. (Note that since we are comparing the width of the typical feature in the azimuthal direction with the thickness in the radial direction, $L\pi/(4\Omega)$ is the correct measure of the characteristic size of the azimuthal variation.) In this regime the $(2+1)D$ cubic self-focusing NLSE

$$i\frac{\partial\psi}{\partial z}+\frac{1}{2}\left\{\frac{\partial^2\psi}{\partial r^2}+\frac{1}{r}\frac{\partial\psi}{\partial r}+\frac{1}{r^2}\frac{\partial^2\psi}{\partial\theta^2}\right\}+|\psi|^2\psi=0, \tag{1}$$

can be approximated as

$$i\frac{\partial\psi}{\partial z}+\frac{1}{2}\left\{\frac{\partial^2\psi}{\partial r^2}+\frac{1}{L^2}\frac{\partial^2\psi}{\partial\theta^2}\right\}+|\psi|^2\psi=0. \tag{2}$$

Thus, one can attempt to write a solution to Eq. (2) as

$$\psi(r,\theta,z)=e^{-i\Gamma z}\sum_{n=1}^{\infty}\sum_{m=1}^{\infty}\{\alpha_{n,m}\cos[(2n-1)\Omega\theta] \times\operatorname{sech}^{2m-1}[(r-L)/w]\}, \tag{3}$$

with $\Gamma(w,L,\Omega)$, $\alpha_{n,m}(w,L,\Omega)$, and Ω is an integer. In this case, there exists a solution like Eq. (3) that has $\alpha_{1,1}$ of $O[(4w\Omega/L\pi)^2]$ larger than any other $\alpha_{n,m}$, and $(\alpha_{1,1})^2 \approx 4/(3w^2)$. Consequently, our intuition tells us that the real solution can probably be well described by

$$\psi(r,\theta,z)=\alpha(z)\cos(\Omega\theta)\operatorname{sech}\{a(z)[r-L(z)]\} \times\exp[-i\Gamma(z)z+iv(z)r], \tag{4}$$

provided that $\alpha^2(z=0)=4a^2(z=0)/3$, $v(z=0)=0$, $w/L \ll 1$, and $w\gg L\pi/(4\Omega)$. We intend to look for $\alpha(z)$, $a(z)$, $L(z)$, $\Gamma(z)$, and $v(z)$ using the action minimization approach. Before proceeding, we emphasize that Eq. (4), when substituted into Eq. (1), produces an undesired singularity at the origin. Consequently, in our simulations, we actually multiply Eq. (4) at the input $(z=0)$ with a smoothly varying function that behaves proportional to r^2 close to the origin, but assumes values close to unity in the regions where most of the energy of Eq. (4) is concentrated. An example of such a function is $\sin^2(r\pi/2L)$. Expanding this function around $r=L(z)$, we conclude that this function's presence influences our action integrals by $O((w/L)^2)$, so we are justified in ignoring its presence when evaluating our integrals; the only place where it actually matters is close to $r=0$, and its only purpose there is to eliminate the singularity. Therefore, when evaluating the action integrals in cylindrical coordinates below, we first integrate over θ, and when integrating over r, we keep in mind that the only important contributions to the integral are close to $r=L(z)$, while the contributions of the regions close to $r=0$ are negligible.

Our Lagrangian density therefore becomes

$$L=i\left\{\psi\frac{\partial\psi^*}{\partial r}-\psi^*\frac{\partial\psi}{\partial r}\right\}+\left(\frac{\partial\psi}{\partial r}\right)\left(\frac{\partial\psi^*}{\partial r}\right) +\frac{1}{r^2}\left(\frac{\partial\psi}{\partial\theta}\right)\left(\frac{\partial\psi^*}{\partial\theta}\right)-|\psi|^4, \tag{5}$$

Using the Lagrangian equations of motion

$$\frac{\partial}{\partial z}\left[\frac{\partial L}{\partial\psi_z^*}\right]+\frac{1}{r}\frac{\partial}{\partial r}\left[r\frac{\partial L}{\partial\psi_r^*}\right]+\frac{\partial}{\partial\theta}\left[\frac{\partial L}{\partial\psi_\theta^*}\right]-\frac{\partial L}{\partial\psi^*}=0, \tag{6}$$

one can obtain Eq. (1) from Eq. (5). In the notation we are using, the action is given by

$$S=\int_{\infty}^{\infty}dz\int_0^{2\pi}d\theta\int_0^{\infty}r\,dr\,L. \tag{7}$$

In order to evaluate the action, we need to evaluate a few integrals. To illustrate how we deal with the singularity at the origin, we present some of the integrals here. For example,

$$\int_0^{\infty}r\times\operatorname{sech}^2[a(r-L)]dr\cong\int_{\infty}^{\infty}(r-L)\operatorname{sech}^2[a(r-L)]dr +\int_{-\infty}^{\infty}L\times\operatorname{sech}^2[a(r-L)]dr =\frac{2L}{a},$$

since the first integrand is odd around $r=L$. Similarly, in the integral $\int_0^{\infty}(dr/r)\operatorname{sech}^2[a(r-L)]$, we can replace

$$\frac{1}{r}=\frac{1}{L}\left\{1-\frac{r-L}{L}+O\left[\left(\frac{w}{L}\right)^2\right]\right\},$$

and integrate from $-\infty$ to ∞ instead, not worrying about what happens at the origin because of the presence of the modulating function which annihilates the singularity, as explained above. The other integrals are evaluated in a similar manner. After a few additional lines of algebra, we obtain

$$S=\pi\int_{-\infty}^{\infty}dz\left\{\frac{4v_z\alpha^2L^2}{a}-\frac{4L\alpha^2}{a}\frac{\partial}{\partial z}[\Gamma z]+\frac{2a\alpha^2L}{3} +\frac{2\alpha^2v^2L}{a}+\frac{2\Omega^2\alpha^2}{aL}-\frac{4L\alpha^4}{3a}\right\}. \tag{8}$$

In order to save ourselves some algebra, we also impose energy conservation for the ansatz in Eq. (4). $E=\int\int|\psi|^2d^2r\cong 2\pi\alpha^2L/a$. We can use this to eliminate $a(z)$ from Eq. (8) in terms of the other variables. We substitute $a=2\pi\alpha^2L/E$ in Eq. (8), where E is a constant. Finally, we require the minimization of the action in Eq. (8) as

$$\frac{\delta S}{\delta\Gamma(\xi)}=\frac{\delta S}{\delta L(\xi)}=\frac{\delta S}{\delta\alpha(\xi)}=\frac{\delta S}{\delta v(\xi)}=0, \tag{9}$$

thereby obtaining $2\pi\alpha L/E=1$, $L_z=v$, and $v_z=(\Omega^2-E^2/12\pi^2)/L^3$ (the subscripts z denote derivatives with respect to z) while the minimization with respect to $\Gamma(\xi)$ does

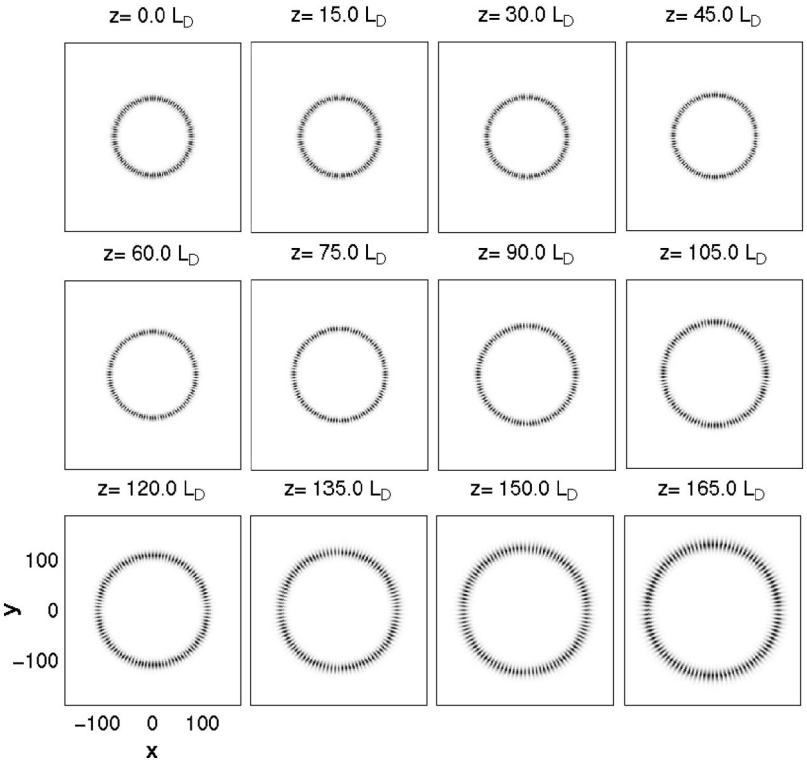

FIG. 3. A necklace whose parameters are in the regime that can be analyzed by the least action principle. At the input of this necklace, $w=5$, $L=76.8$, $\Omega=50$, and $\alpha^2=4/(3w^2)$. The analytical solutions we find approximate the subsequent evolution of the shape of this necklace to within a few percent. The regime that can be understood analytically is described by the parameters that satisfy $\alpha^2=4/(3w^2)$, $w/L\ll 1$, and $L\pi/(4\Omega)\ll w$.

not yield any useful result. From these equations we also obtain $a=E/(2L\pi)$. Integrating these ODEs we obtain

$$L(z)=\sqrt{\left[\frac{1}{L_0^2}\left(\Omega^2-\frac{E^2}{12\pi^2}\right)+v_0^2\right]z^2+2L_0v_0z+L_0^2}, \tag{10}$$

where the subscript zero denotes the initial conditions at $z=0$.

Note that our ansatz therefore describes a solution whose intensity and shape scale simply as a function of z, preserving the total energy as the necklace expands, which is consistent with our intuition from Ref. [5].

To test our analytical results, we simulate the evolution of a few necklaces using the split-step Fourier method and we compare the necklace beams evolving (expanding) during propagation with the approximate analytic solution presented in Eq. (4). Given the insight provided by Eq. (3), we expected to obtain the best results when our input conditions were

$$\psi(r,\theta,z=0)=\alpha\cos(\Omega\theta)\mathrm{sech}\{[r-L]/w\}, \tag{11}$$

where $\alpha^2=4/(3w^2)$, $w/L\ll 1$, and $L\pi/(4\Omega)\ll w$. Note that the solution from Eq. (4) satisfies Eq. (1) best if the initial radial velocity, $v(z=0)=0$, so we take it to be zero. Further, in the simulations, the input waveform given by Eq. (11) is multiplied by $\sin^2(\pi r/2L)$ in order to eliminate the singularity at the origin. Nevertheless, as explained above, this modulation to a very good approximation has no other influence on subsequent dynamics or necklace shape. For the example presented in Fig. 3, $L=76.8$, $w=5$, and $\Omega=50$. At the output of the propagation, after $z=165$, the width of the necklace is $L=130.04$. The intensity overlap of the final necklace (which evolved throughout propagation) with the approximate necklace solution given by Eq. (4) that had $L=130.04$ was approximately 97%. In other words, if we denote the final necklace with ψ_1, and the approximate necklace solution with ψ_2, we get that the overlap is

$$\frac{\int\int d^2r\,|\psi_1|^2-|\psi_2|^2|}{\int\int d^2r\{|\psi_1|^2+|\psi_2|^2\}}\approx 0.03. \tag{12}$$

Furthermore, we check our prediction for $L(z)$ as given by Eq. (10) against our numerical simulations. The result presented in Fig. 4 shows a very good agreement between the analytic (approximate) prediction and direct simulation.

In addition to these excellent agreements (between the analytics and the numerics) in the shape and the radius of the necklaces, we measure the radial velocity $v(z=165)$ of the

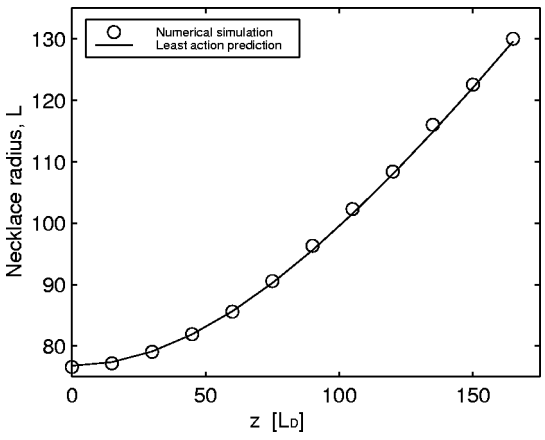

FIG. 4. Predicting the instantaneous necklace radius of the necklace from Fig. 3, using the least action principle.

necklace at the output, and find that it disagrees with the prediction given by Eq. (10) by less than 3%. Furthermore, we take the output at $z=165$, and multiply the whole shape with $\exp\{-iv(z=165)r\}$. According to our analytical predictions, this should have reduced the instantaneous radial velocity of the necklace to zero. Indeed, it reduced the instantaneous radial velocity to less than 2.5% of its initial value.

To conclude this section, the agreement between the analytical theory and the numerical results is very good. Since we expect our results to be valid only to $O\{[L\pi/(4\Omega w)]^2\}$, or $O[(w/L)^2]$, one should not have expected the agreement to be better than O(few%) for the particular necklace presented in Fig. 3.

Unfortunately, our analytical solution works only when the required smallness parameters are truly small. In particular, $[L\pi/(4\Omega w)]^2=1/17.18$, and $(w/L)^2=1/236$ for the necklace of Fig. 3. When the required smallness parameters are closer to unity, one can probably still obtain reasonable analytical solutions by including more terms from the expansion in Eq. (3) (rather than including only the lowest-order terms) into the ansatz of Eq. (4). However, one of the requirements for the stability of any necklace beam is that the azimuthal width of the pearls has to be of the same order or smaller than the radial width of the pearl. In addition, the radius of any necklace should be significantly larger than its thickness. Therefore, typical stable necklace-ring beams that we expect to be stable in self-focusing Kerr media naturally have the required parameters small, which makes the proposed expansion seem promising. Extending the regime of validity of our approximate method by including higher-order terms is beyond the scope of this paper, and we leave it to future research.

V. PREDICTING AND CONTROLLING THE EXPANSION RATES OF ARBITRARY SELF-TRAPPED NECKLACES

As shown in the preceding section, an excellent analytical solution for self-trapped necklace beams can be found in certain regimes of parameters. However, the approach of the preceding section does not work in some rather interesting regimes of necklace parameters; consequently, we are not able to write down the explicit analytical solution in those regimes. In this section we present another analytical approach that gives a good prediction for the radius of the necklace as a function of the initial necklace shape and the propagation distance. This approach works even though one does not know the instantaneous analytical solution for the necklace shape. It can also be used to predict the dynamics of a necklace after multiplication with an arbitrary radial phase. But, this approach below works *only* for the $(2+1)D$ self-focusing cubic NLSE, whereas the approach from Sec. IV seems to be adaptable for any number of dimensions, and for any form of nonlinearity. In any case, it is worthwhile to present both approaches in this paper, and also to use them as a mutual check on each other.

We follow the approach given in [16,17] to derive the instantaneous radius of the necklace radius as a function of the propagation distance, and the initial necklace shape. First, we need to define the energy

$$E=\int\int_{\text{space}} d^2x|\psi(z=0)|^2, \tag{13}$$

and also the Hamiltonian

$$H=\int\int d^2x\{(\nabla\psi(z=0))\cdot(\nabla\psi^*(z=0))-|\psi(z=0)|^4\}. \tag{14}$$

Both E and H are conserved. Energy is conserved because of the symmetry of Eq. (1) with respect to a phase shift. The Hamiltonian is conserved because of the invariance of Eq. (1) with respect to a shift in z. Therefore, using Noether's theorem one can prove that E and H as defined in Eqs. (13) and (14) are conserved (alternatively, one can use the method given in Ref. [4] to show this). Defining

$$R^2(z)\equiv\frac{1}{E}\int\int d^2x\{|\psi(z)|^2r^2\}, \tag{15}$$

after a few lines of algebra, one can show

$$\frac{d^2[R^2(z)]}{dz^2}=2\frac{H}{E}, \tag{16}$$

which thus provides us with another very useful conserved quantity. Defining the local current in the usual way,

$$\mathbf{j}(r,\theta,z)\equiv\frac{i}{2}\{\psi(r,\theta,z)\nabla\psi^*(r,\theta,z)-\psi^*(r,\theta,z)\nabla\psi(r,\theta,z)\}, \tag{17}$$

one can show that

$$\frac{d[R^2(z)]}{dz}=\frac{2}{E}\int\int_{\text{space}} d^2x\{\mathbf{j}(r,\theta,z)\cdot\mathbf{r}\}. \tag{18}$$

Therefore, given the initial condition $\psi(r,\theta,z=0)$, we can integrate Eq. (16) to obtain

$$R^2(z)=\frac{H}{E}z^2+\frac{2z}{E}\int\int_{\text{space}} d^2x\{\mathbf{j}(r,\theta,z=0)\cdot\mathbf{r}\}+R^2(z=0). \tag{19}$$

How can we use this result? Well, if it is a valid assumption that most of the initial necklace energy stays bound to the necklace as the necklace propagates (i.e., only a negligible amount of E and H are carried away from the necklace as the necklace propagates, as we fully expect from self-trapped propagation and as we have found numerically in [5] and in the examples in this paper), then Eq. (19) lets us predict the instantaneous necklace radius $L(z)$. [By $L(z)$ we mean the distance from the origin where $|\psi(r,\theta,z)|$ is largest; see Fig. 1.] This is because it is trivial to show that for typical necklaces $L(z)\approx\sqrt{R^2(z)}$ up to $O(w^2/L^2)$ as long as w/L is small, which is naturally satisfied by all self-trapped necklaces of interest (i.e., those that propagate in a stable fashion in Kerr media).

It is now instructive to compare the prediction from Eq. (19) with the prediction we obtained using the action minimization approach in Sec. IV, like Eq. (10). Adapting Eq. (19) for the necklace of Fig. 3, we find

$$L(z)\approx\sqrt{R^2(z)}=\sqrt{\left[\frac{1}{L_0^2}\left(\Omega^2-\frac{3E^2}{64\pi^2}\right)\right]z^2+R_0^2}. \quad (20)$$

Comparing this with Eq. (10), after setting $v_0=0$ in that equation, we see that the relative error in the term proportional to z^2 is $7E^2/(192\pi^2\Omega^2)=7L_0^2/(27\Omega^2)w^2$, which is tiny for that necklace. Similarly, as we have already shown, the error in the term proportional to z^0 is $O(w^2/L^2)$ which is again negligible. Extending this analysis for the cases where $v_0\neq 0$ is a bit more involved, but the result is again that the two approaches differ only by a tiny amount which is set by the smallness parameters of the necklace.

In order to test our results, we simulate numerically several typical examples of self-trapped necklaces and compare them with the prediction given by Eq. (19). We obtain best results if the initial shapes are as close to the true ''equilibrium'' shape as possible, because in that case only a negligible amount of energy is carried away with radiation through subsequent breathing of the necklace. (In other cases, some energy is lost to radiation in the formation process of the necklace, as always occurs in the formation of solitons from a nonperfect input.) However, since there are no analytical solutions for necklaces in all regimes, a typical necklace at the input is only an approximation to the equilibrium necklace shape. Nevertheless, this technique gives us a good prediction of the subsequent necklace dynamics, provided that not much energy is eventually scattered into radiation. In any case, experimentally, all necklaces are expected to be launched with a $\psi(z=0)$ real, so $L(z)\approx\sqrt{(H/E)z^2+L^2(z=0)}$. Our necklaces at the input are given by

$$\psi(r,\theta,z=0)=\alpha\cos(\Omega\theta)\operatorname{sech}\left(\frac{r-L}{w}\right)\sin^2\left(\frac{r\pi}{2L}\right), \quad (21)$$

where $L/\Omega=1.7072$, $w=1$, and $\alpha=1$; according to our experience this input shape is close to the equilibrium necklace shape. As examples, we consider the cases where $\Omega=4$, 8, 16, and 32. The purpose of the $\sin^2$ term in Eq. (21) is again only to eliminate the singularity at the origin; we can ignore this term when performing the relevant integrals, as we did in Sec. IV, since the relative mistake is only $O(w^2/L^2)$ which is negligible for our necklaces. All the relevant integrals needed to obtain the Hamiltonian and energy are evaluated in exactly the same manner as in Sec. IV. Therefore, we obtain

$$L(z)\sim\sqrt{\left\{\frac{1}{3w^2}+\frac{\Omega^2}{L^2}-\frac{\alpha^2}{2}\right\}z^2+L^2(z=0)}. \quad (22)$$

For each of the necklaces, we compare the prediction given by Eq. (22) with the actual numerical experiment. The result is shown in Fig. 5. The circles represent numerical data, while the solid lines represent the predictions given by Eq. (22). As we can see, our analytical prediction is a fairly good approximation for reasonable propagation distances (a few tenths of diffraction lengths). Keeping in mind that the largest propagation distance observed so far for spatial solitons is roughly $20L_D$; being able to make analytical predictions up to a distance of $30L_D$ is very useful. However, the real value of the prediction in Eq. (22) is that it gives a good estimate

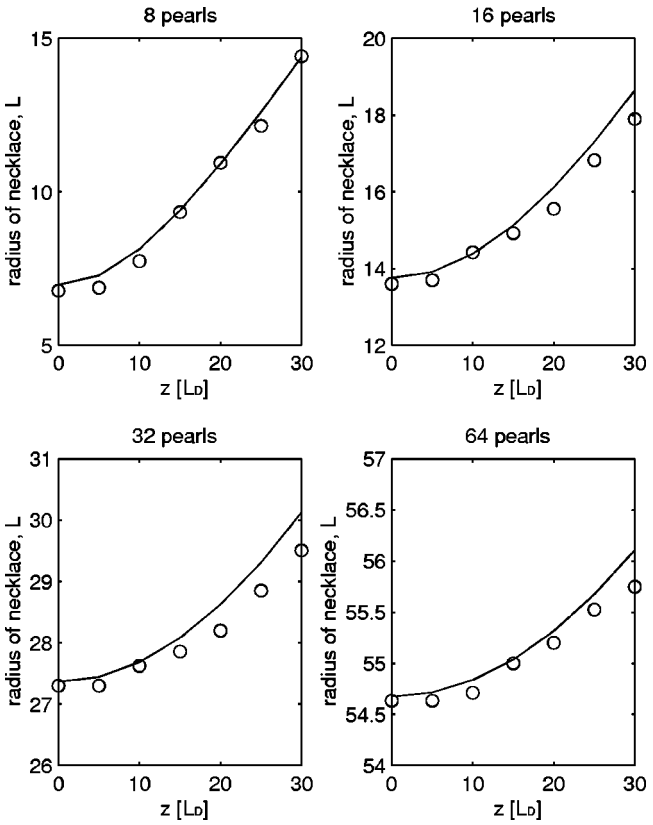

FIG. 5. Predicting the expansion rates of arbitrary self-trapped necklaces: comparison between numerical beam-propagation results and analytical predictions. All necklaces here have $L/\Omega=1.707$, $\alpha=1$, and $w=1$. Their respective $\Omega=4$, 8, 16, and 32. The analytical approach used here is based on using some conservation laws of the $(2+1)D$ cubic NLSE, in order to find the instantaneous necklace radius directly. This approach works for a necklace of arbitrary parameters as long as most of its initial energy and Hamiltonian are self-trapped to the necklace as it propagates.

for the dynamics even for necklace beams whose shape is not initially very close to the existence curve. For example, we launch a few necklaces that have very similar dimensions to those in Fig. 5, but with a Gaussian instead of a sech shape at the input. This shape is not close to the equilibrium necklace shape; nevertheless, the agreement between the numerical results and the analytical predictions for the expansion of the necklace beams is still reasonably good, as shown in Fig. 6.

Now that we have an analytical expression for the necklace dynamics, as given by Eq. (22), we can study the feasibility of making a stationary necklace. That is, we would like to know whether it is possible to construct a necklace that would not change its radius at all as it propagates. Looking at Eq. (22) it seems that all we have to do is construct a necklace whose parameters make the term proportional to z^2 in Eq. (22) to zero. For example, we can fix $w=\alpha=1$, and pick L that will make the given term zero. However, in that case we conclude that the azimuthal width of each pearl, $L\pi/(4\Omega)=1.92$, which is bigger than the radial width of the pearl, and therefore such necklace beam is not stable in self-focusing Kerr media. For the given intensity, the pearl will self-focus in the azimuthal direction, and this will eventually destabilize the necklace and disintegrate it. We run the simulation with these precise parameters, and our expectations

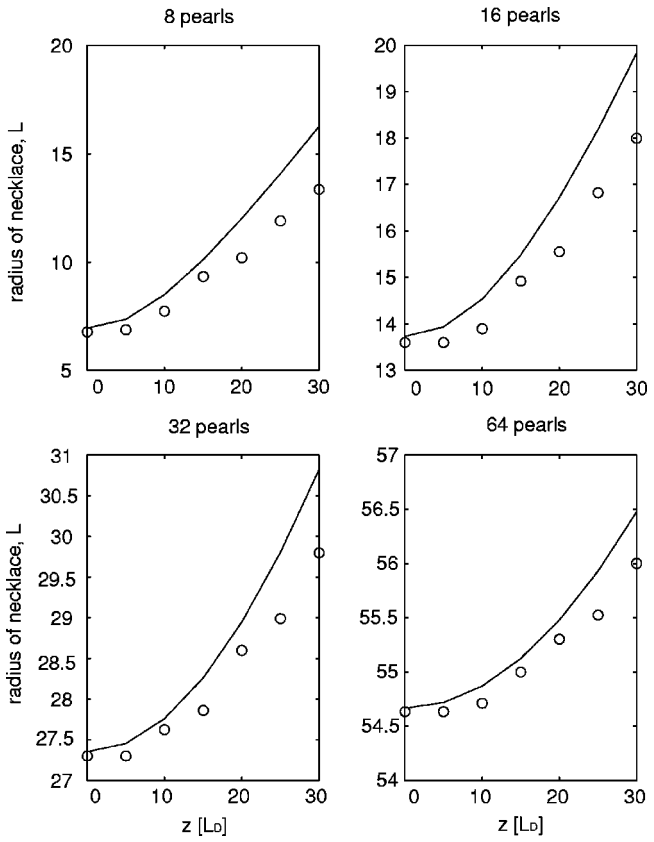

FIG. 6. Predicting the expansion rates of arbitrary necklaces whose shapes are not close to the equilibrium shapes initially. These necklaces have the same full width at half maximum, radiuses, energies, and Ωs as their counterparts in Fig. 5. But, their radial profiles are initially Gaussian instead of sech shaped. Thus, they are not close to the equilibrium self-trapped shapes. Nevertheless, the analytic approach used in Fig. 5 still gives a useful approximation when predicting the radial necklace dynamics.

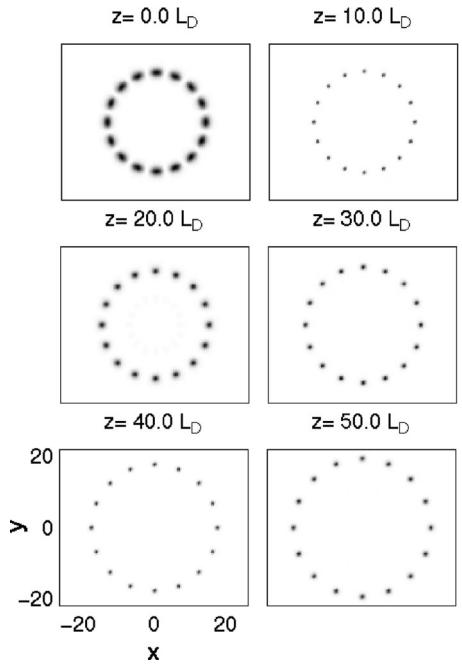

FIG. 7. A necklace with no radial dynamics. Our analytical understanding of radial dynamics of necklaces lets us design a necklace whose radius is stationary as the necklace propagates. The necklace presented here has $\alpha=1.16$, $w=1$, $\Omega=8$, and $L/\Omega=1.707$. Unfortunately, this necklace has α far away from the equilibrium shape. Thus, each pearl has its own dynamics that eventually [after $O(40L_D)$] destabilizes the necklace. Nevertheless, as long as the necklace is stable [until $O(40L_D)$], its radius does not change as was predicted by our analytics.

were confirmed. The radius of the necklace does not change almost at all. However, each pearl keeps shrinking in the azimuthal direction, and the necklace destabilizes within $O(40L_D)$. Therefore, setting $w=\alpha=1$ and choosing an L that eliminates the term proportional to z^2 in Eq. (22), yields a nonexpanding necklace that is basically unstable but can survive for tens of L_D's. Another option to stop the expansion is to increase only α. We take the necklace from Fig. 1, and keeping all of its other parameters fixed, we increase α till the term proportional to z^2 in Eq. (22) vanishes. Unfortunately, the necessary α is equal to 1.16, which is too far off the equilibrium necklace shape. As shown in Fig. 7, this alternative also leads to nonstationary propagation because the pearls keep shrinking, even though the necklace radius is largely unchanged till $O(40L_D)$. Thus, choosing parameters so that the term proportional to z^2 in Eq. (22) is set to zero seems not to be a fully satisfactory method for stopping the necklace expansion.

Even though the structure in Fig. 7 is clearly nonstationary, there are important lessons to be learned from it. The first lesson is that our analytical expression Eq. (22) seems to work well, giving correct predictions even when the initial shapes are far away from the equilibrium necklace shapes. Furthermore, by increasing the azimuthal width of each pearl a little, and also increasing the peak amplitude slightly, one could produce a necklace beam that would be stable and stationary for a fairly long distance, say $O(40L_D)$. Eventually, the necklace would disintegrate since its initial shape would be too far away from the equilibrium necklace shape [18]. However, the propagation distance during which such a necklace is stable is sufficient for experimental interest and its conditions are not too stringent. Finally, as the result from Fig. 7 clearly demonstrates, our previous intuition, that the force holding the necklace together results from repulsion between adjacent ''pearl'' solitons, needs to be reexamined more carefully. In particular, Eq. (22) implies that by choosing the proper parameters, one can make both the initial radial velocity and the initial radial acceleration of the necklace to be negative. Sure enough, such a necklace eventually turns out to be unstable, but this fact does not diminish the fact that the necklace is held together by a force that is not net repulsion only. One can think about this force as ''surface tension,'' yet thus far the analogy is not really substantiated.

We now proceed to use the analytical tools from above to analyze what happens if one introduces an arbitrary radial phase to any necklace, at an arbitrary moment z_0. In particular, we assume $\psi(r,\theta,z_{0+})=\psi(r,\theta,z_0)\exp(ivr)$, where z_{0+} denotes the moment immediately after imposing the radial phase, and z_0 denotes the moment immediately before. After a few lines of algebra, we get $E(z_0)=E(z_{0+})$, and also

$$\left.\frac{d[R^2(z)]}{dz}\right|_{z_{0+}}=\left.\frac{d[R^2(z)]}{dz}\right|_{z_0}+\frac{2v}{E}\int\int_{\text{space}} d^2x|\psi(z_0)|^2 r. \tag{23}$$

Note that for typical necklaces the last term in Eq. (20) is very close to $2vL(z_0)$. Approximating $L^2(z) \approx R^2(z)$ in Eq. (23), we therefore obtain

$$\left.\frac{dL(z)}{dz}\right|_{z_{0+}} = \left.\frac{dL(z)}{dz}\right|_{z_0} + v, \tag{24}$$

which is exactly as expected. Furthermore, we can also find out what happens with the Hamiltonian after imposing this radial phase

$$H(z_{0+}) = H(z_0) + v^2 E + 2v \int_{\text{space}} \int d^2x \{\mathbf{j}(r,\theta,z_0)\cdot\hat{\mathbf{r}}\}. \tag{25}$$

Since the last term in Eq. (25) is negative for a negative radial phase, it is not clear whether imposing a radial phase in order to stop the instantaneous radial expansion would typically decrease or increase the Hamiltonian. Thus, we do not know how would it influence the term proportional to z^2 in Eq. (19). Note that this term is related (but not equal) to the instantaneous radial acceleration of each pearl. To proceed with our analysis, we assume that at the input $(z=0)$ we start with a necklace beam that has zero radial velocity. Then, we propagate the necklace for some z_0, at which point according to our analysis in Eq. (19), its radial velocity should be given by approximately $v_0 = Hz_0/[EL(z_0)]$. Therefore, we multiply the whole shape with $\exp(-iv_0 r)$. Then, we notice the similarity between the last term in Eq. (25), and the Eq. (18) to conclude

$$H(z_{0+}) = H(z_0)\frac{L^2(z=0)}{L^2(z=z_0)}. \tag{26}$$

This is telling us that after imposing the radial phase, the necklace will have the same dynamics as the scaled-up version of the necklace we started with at $z=0$. This is consistent with our picture from Ref. [5] that the intensity of the necklace to a good approximation simply scales as the necklace propagates, according to the rescaling properties of Eq. (1) which conserve the energy in the beam. Notice that in addition to extinguishing the instantaneous radial velocity, we have also slowed down the subsequent dynamics, as one can see by comparing Figs. 1 and 2. In a way, this is expected, because it is natural that a scaled-up necklace would have a slower dynamics, exactly by the factor given in Eq. (26).

By imposing a large enough negative radial phase, the radial acceleration can in principle be turned into zero, or even negative. But, this is not a stable solution because the radial phase needed to obtain this is huge compared to other necklace parameters, making this proposal infeasible. Also, in that case the necklace would keep contracting until it destroys itself (each pearl undergoes the equivalent of catastrophic collapse). Consequently, in typical experimental realizations, one would probably want to let the necklace expand for a while, then impose a large enough negative radial phase to make it contract for a while, until it starts expanding again. Then one would impose a negative radial phase again, etc.

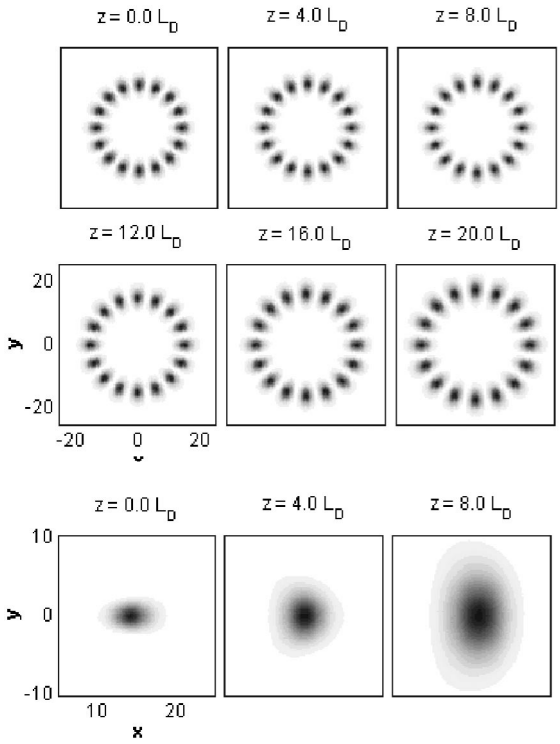

FIG. 8. (a) The radial dynamics of a necklace. The initial necklace shape is $\psi(r,\theta,z=0) = 0.56\,\mathrm{sech}[(r-13.66)/2]$ (times a modulation function that removes the singularity at the origin while leaving everything else unchanged). As shown here, this necklace has a rather slow radial dynamics. (b) The propagation dynamics of a single pearl taken from the self-trapped necklace of (a) after $8L_D$. Shown are the dynamics of the isolated rightmost pearl. As shown here, a stand-alone pearl diffracts (expands) much faster than the expansion dynamics of the whole necklace [as shown in the bottom row of (a)].

VI. CONCLUSION

We revisit self-trapped necklace-ring beams in self-focusing Kerr media, and, with collision experiments in mind, we investigate the possibility of controling the dynamics of these structures. Using the action minimization approach, we find analytical solutions for the necklace shapes in specific regimes of necklace parameters, and present analytical techniques for predicting the radial dynamics of a necklace of any arbitrary initial shape, even if the shape is not close to the equilibrium necklace shape. We also present a procedure that enables us to control and reverse the instantaneous necklace radial dynamics. All the tools that we presented in this paper enable us to design many different necklaces which are essentially stationary over most propagation distances of physical interest: tens of diffraction lengths. Such self-trapped necklaces resemble solitons in many ways: a necklace conserves energy and momentum and does not change its shapes over the experimentally reachable propagation distances. Therefore, for all practical purposes, we can treat the self-trapped necklaces as ''quasisolitons'' of the $(2+1)D$ self-focusing cubic NLSE. This is in sharp contrast to the previously held belief that this equation does not support solitons. Consequently, as an avenue of further research, we envision studying all solitonic effects with necklaces,

both experimentally and theoretically, including interactions of such necklaces. Finally, we emphasize that this work on self-trapped necklace-ring beams is of direct relevance and should be observable in all other nonlinear systems described by the cubic $(2+1)D$ nonlinear Schrödinger equation: practically in almost all centrosymmetric nonlinear systems in nature that describe envelope waves [3].

ACKNOWLEDGMENTS

The work at Princeton University was supported by the U.S. Army Research Office and by the NSF. The work in Israel was supported by the Israeli Ministry of Science.

APPENDIX

As mentioned in the text, it is a well known fact that cylindrically symmetric bright solitons of $(2+1)D$ Kerr NLSE are unstable. If their power is above the so-called critical power, they undergo catastrophic collapse, and if the power is below the critical power, they diffract [4]. Each pearl (bright spot) in a typical necklace that exhibits stable self-trapped propagation has a power that is slightly below the critical power, thus, the necklace slowly expands as it propagates. (If the power in this necklace is increased, as shown in Fig. 7, each pearl in the necklace shrinks and becomes unstable.) However, it is important to appreciate that this radial dynamics of a stable necklace is much slower than what the growth rate of each pearl would be if the pearl was standing by itself. The reason for this is that the stabilizing mechanism for a pearl in a necklace is much different than for a pearl standing by itself. If a pearl is standing alone, it has to be self-trapped in both dimensions by its self-trapping. However, if it is in a necklace, the self-focusing traps it (arrests the expansion) in the radial direction only. (In the azimuthal direction, the expansion is arrested by the repulsion from the neighboring pearls.) Recalling that stable self-trapping in Kerr media is possible in one dimension, but not in two dimensions, this explains why a pearl is stable in a necklace but not when standing alone. In fact, since the azimuthal length of the pearl is smaller than the radial length (and the peak intensity is chosen just right to provide self-trapping in the radial direction), the self-focusing effects in the azimuthal direction cannot compensate for the pearl's tendency to expand in the azimuthal direction. Therefore, each pearl is far from being independent; the presence of the other pearls is crucial for arresting the azimuthal expansion of each pearl. To check this hypothesis, we take a necklace from Fig. 8(a), and after $8L_D$, we remove all the pearls except the rightmost one. The subsequent development of this pearl (when standing alone), is shown in Fig. 8(b), which confirms that it is the mutual interaction among the pearls that leads to self-trapping of the necklace as a whole.

[1] M. Segev and G. I. Stegeman, Phys. Today **51** (8), 42 (1998).

[2] For a list of reviews on solitons in physics and mathematics see A. Degasperis, Am. J. Phys. **66**, 486 (1998).

[3] E. Infeld and G. Rowlands, *Nonlinear Waves, Solitons and Chaos* (Cambridge University Press, Cambridge, UK, 1990), Chap. 5 (in particular p. 127).

[4] See, e.g., N. N. Akhmediev, Opt. Quantum Electron. **30**, 535 (1998) and references therein.

[5] M. Soljačić, S. Sears, and M. Segev, Phys. Rev. Lett. **81**, 4851 (1998).

[6] Just before this current paper was submitted, we were informed by Professor Alain Barthelemy that his group had in fact observed self-trapped necklaces in Kerr media back in 1993, yet they had trouble publishing it. Therefore, it has appeared in conference proceedings only. See A. Barthelemy, C. Froehly, and M. Shalaby, SPIE International Symposium on Optics, Quebec, 1993 [J. Soc. Photo-Opt. Instrum. Eng. **2041**, 104 (1993)]. At the time Ref. [5] was published, we had no idea about Barthelemy's experiments.

[7] A recent observation of necklace-ring solitonlike patterns was made in a two-dimensional array of vertical cavity surface emitting lasers, and reported by J. Scheuer, D. Arbel, and M. Orenstein, *Nonlinear Guided Waves and Their Applications Conference* (Optical Society of America, Washington, DC, 1999), pp. 180–182. The nonlinear medium involved is NOT a Kerr medium, but rather a (resonant) laser medium, so the underlying equation is the complex Ginzburg-Landau equation and not the cubic NLSE as in [5] and in the present work. Nonetheless, the observed necklace-ring solitons in both cases seem to have many features in common.

[8] See, e.g., H. A. Haus, Appl. Phys. Lett. **8**, 128 (1966).

[9] P. L. Kelley, Phys. Rev. Lett. **15**, 1005 (1965).

[10] V. E. Zakharov and A. M. Rubenchik, Zh. Eksp. Teor. Fiz. **65**, 997 (1973) [Sov. Phys. JETP **38**, 494 (1974)].

[11] Azimuthal modulation instability of uniform bright ring beams (carrying zero topological charge) in self-focusing Kerr media was demonstrated theoretically by Y. Chen and A. W. Snyder, Europhys. Lett. **27**, 565 (1992); Y. Chen, IEEE J. Quantum Electron. **QE-26**, 1236 (1991). See also Fig. 4 in Ref. [5]. To our knowledge, this instability has not yet been observed experimentally in Kerr media. Uniform bright ring beams with zero topological charge are azimuthally unstable also in saturable self-focusing media as shown theoretically by J. Atai, Y. Chen, and J. M. Soto-Crespo, Phys. Rev. A **49**, R3170 (1994).

[12] Azimuthal modulation instability of bright ring beams that carry nonzero topological charge, in self-focusing (Kerr and non-Kerr) media was demonstrated theoretically by several groups, including V. I. Kruglov, Y. A. Logvin, and V. M. Volkov, J. Mod. Opt. **39**, 2277 (1992); W. J. Firth and D. V. Skryabin, Phys. Rev. Lett. **79**, 2450 (1997); L. Torner and D. V. Petrov, Europhys. Lett. **33**, 608 (1997); J. Opt. Soc. Am. B **14**, 2017 (1997), and others. The vortex-ring beam disintegrates into multiple *isolated* filaments. In Kerr media, the isolated filaments are of course unstable. In saturable self-focusing media, the filaments are stable and can interact with one another (if they are close enough to each other) or simply move outwards like free particles. Experimentally, disintegration of vortex-ring beams in saturable self-focusing media was observed by V. Tikhonenko, J. Christou, and B. Luther-Davies, Phys. Rev. Lett. **76**, 2698 (1996); J. Opt. Soc. Am. A **12**, 2046 (1995) in atomic vapor and by Z. Chen, M. Shih, M. Segev, D. W.

Wilson, R. E. Muller, and P. D. Maker, Opt. Lett. **22**, 1751 (1997) in photorefractives. To our knowledge, the disintegration of vortex-ring beams in self-focusing Kerr media was not observed experimentally yet.

[13] J. S. Aitchison, A. M. Weiner, Y. Silberberg, M. K. Oliver, J. L. Jackel, D. E. Leaird, E. M. Vogel, and P. W. Smith, Opt. Lett. **15**, 471 (1990).

[14] A. Barthelemy, S. Maneuf, and C. Froehly, Opt. Commun. **55**, 201 (1985).

[15] D. J. Mitchell, A. W. Snyder, and L. Poladian, Phys. Rev. Lett. **77**, 271 (1996).

[16] L. D. Landau and E. M. Lifshitz, *Electrodynamics of Continuous Mediua*, 2nd ed. (Butterworth-Heinenann, Oxford, 1982), Chap. XIII, p. 382.

[17] V. V. Afanasjev, Phys. Rev. E **52**, 3153 (1995).

[18] Interestingly, in our simulations, we never find a nonexpanding necklace that remains stable forever, we were able to adjust and optimize the necklace parameters so that it is nonexpanding and remains stable for a longer distance, but such fine tuning is most probably beyond experimental relevance. What we show in Fig. 7 is an example where the fine tuning is within reasonable experimental reach.